Direct target and non-target analysis of urban aerosol sample extracts using atmospheric pressure photoionisation high-resolution mass spectrometry

Accepted Manuscript

Direct target and non-target analysis of urban aerosol sample extracts using atmospheric pressure photoionisation high-resolution mass spectrometry

Chiara Giorio, Claudio Bortolini, Ivan Kourtchev, Andrea Tapparo, Sara Bogialli, Markus Kalberer

PII: S0045-6535(19)30375-3

DOI: https://doi.org/10.1016/j.chemosphere.2019.02.151

Reference: CHEM 23263

To appear in: *ECSN*

Received Date: 18 October 2018

Revised Date: 21 February 2019

Accepted Date: 22 February 2019

Please cite this article as: Giorio, C., Bortolini, C., Kourtchev, I., Tapparo, A., Bogialli, S., Kalberer, M., Direct target and non-target analysis of urban aerosol sample extracts using atmospheric pressure photoionisation high-resolution mass spectrometry, *Chemosphere* (2019), doi: https://doi.org/10.1016/j.chemosphere.2019.02.151.

Direct target and non-target analysis of urban aerosol sample extracts using atmospheric pressure photoionisation high-resolution mass spectrometry

Chiara Giorio[1,2*], Claudio Bortolini[2], Ivan Kourtchev[1], Andrea Tapparo[2], Sara Bogialli[2], Markus Kalberer[1,3]

[1] Department of Chemistry, University of Cambridge, Lensfield Road, Cambridge, CB2 1EW, United Kingdom
[2] Department of Chemical Sciences, University of Padua, via Marzolo 1, Padova, 35131, Italy
[3] Department of Environmental Sciences, University of Basel, Klingelbergstrasse 27, 4056 Basel, Switzerland

* Correspondence to: chiara.giorio@unipd.it

Abstract (max 250 words)

Polycyclic aromatic hydrocarbons (PAHs) are ubiquitous atmospheric pollutants of high concern for public health. In the atmosphere they undergo oxidation, mainly through reactions with ·OH and NOx to produce nitro- and oxygenated (oxy-) derivatives. In this study, we developed a new method for the detection of particle-bound PAHs, nitro-PAHs and oxy-PAHs using direct infusion into an atmospheric pressure photoionisation high-resolution mass spectrometer (APPI-HRMS). Method optimisation was done by testing different source temperatures, gas flow rates, mobile phases and dopants. Samples were extracted with methanol, concentrated by evaporation and directly infused in the APPI source after adding toluene as dopant. Acquisition was performed in both polarity modes. The method was applied to target analysis of seasonal $PM_{2.5}$ samples from an urban background site in Padua (Italy), in the Po Valley, in which a series of PAHs, nitro- and oxy-PAHs were detected. APPI-HRMS was then used for non-target analysis of seasonal $PM_{2.5}$ samples and results compared with nano-electrospray ionisation (nanoESI) HRMS. The results showed that, when samples were characterised by highly oxidised organic compounds, including S-containing compounds, like in summer samples, APPI did not bring any additional information with respect to nanoESI in negative polarity (nanoESI(-)). Conversely, for winter samples, APPI(-) could detect a series of aromatic and poly-aromatic compounds, mainly oxidised and nitrogenated aromatics, that were not otherwise detected with nanoESI.

Keywords (4-6 keywords)

APPI-MS, nanoESI-MS, HRMS, $PM_{2.5}$, urban background, PAH derivatives

1 Introduction

Polycyclic aromatic hydrocarbons (PAHs), organic compounds with two or more fused aromatic rings, are ubiquitous atmospheric pollutants, produced by incomplete combustion and pyrolysis of both biomass and fossil fuel (Srogi, 2007; Valotto et al., 2017). PAHs are highly carcinogenic and/or mutagenic (Kim et al., 2015; Srogi, 2007; Zhang et al., 2015). Low molecular weight PAHs (e.g. 2-3 rings) have a higher concentration in the gas phase, whereas those with high molecular weight are often found as particle-bound components (Stracquadanio and Trombini, 2006; Valotto et al., 2017).

The northern Italian Po valley represents a hot spot in Europe concerning air pollution (Masiol et al., 2013; Stracquadanio et al., 2007), with concentration values of particle-bound PAHs often exceeding the levels targeted by the European legislation (Masiol et al., 2013; Stracquadanio et al., 2007), as 1 ng/m^3 of benzo[a]pyrene averaged over a calendar year (EU, 2005).

In the atmosphere, PAHs and particle-bound PAHs can undergo photochemical ageing. They can react in the gas phase or through heterogenous reactions with hydroxyl radical (·OH), nitrate radical ($\cdot NO_3$), nitrogen oxides (NOx), and (for olefinic PAHs) ozone (O_3) to form nitro and oxygenated derivatives (nitro-PAHs and oxy-PAHs) (Nyiri et al., 2016). Nitroaromatic compounds are known chromophores, able to reduce near-UV irradiance within the boundary layer (Laskin et al., 2015). Specifically, nitrated PAHs are able to absorb UV light and are therefore constituents of the brown carbon fraction of the aerosol having a direct impact on the Earth's climate (Laskin et al., 2015).

The official method for the determination of PAHs in aerosol sampled on filters includes extraction with a Soxhlet apparatus using a diethyl ether/*n*-hexane mixture or dichloromethane for 14-24 h, followed by concentration of the extract in a Kuderna-Danish concentrator. The extract is then analysed with gas chromatography mass spectrometry (GC-MS) (ASTM International, 2013). Such method includes a time-consuming sample preparation procedure which could be replaced by faster and more efficient methods. Lim et al., (2013) used pressurised liquid extraction with

toluene/methanol (9:1) for 43 PAHs which were then determined using 2D-LC/2D-GC/MS. However, the most commonly used method of analysis of aerosol samples for the determination of PAHs uses LC-fluorimetry (Stracquadanio et al., 2007) which can be used after a simple and fast sample extraction method using acetonitrile as extraction solvent in ultrasonic bath, followed by evaporation of the solvent to concentrate the extract (Bacaloni et al., 2004). While fluorimetry is often the detection technique of choice for unsubstituted PAHs, nitro- and oxy-PAHs are not amenable to fluorescence detection without a derivatisation step (Delhomme et al., 2007) and may be detected more efficiently with MS techniques (Niederer, 1998).

Nyiri et al. (2016) optimised a sample preparation method in which extraction was done in *n*-hexane *via* sonication, followed by clean up through water addition, centrifugation, recovery of the organic fraction, anhydrification, and evaporation down to 2 mL. After that, 1 mL of the extract was analysed for PAHs and oxy-PAHs, with GC-MS. The other aliquot was treated with dimethyl sulfoxide, evaporated down, and recovered with 1 mL of acetone for determination of nitro-PAHs with liquid chromatography atmospheric pressure chemical ionisation mass spectrometry (LC-APCI-MS). Adelhelm et al. (2008) used LC coupled with both APCI and atmospheric pressure photoionisation (APPI) MS for analysis of oxy- and nitro-PAHs. Sample extraction was done in an ultrasonic bath with a mixture of toluene, dichloromethane, and methanol, followed by evaporation to dryness, recovery with toluene, silica-column clean-up, evaporation to dryness and reconstitution with methanol. Grosse and Letzel (2007) also used LC-APPI-MS for quantification of oxy-PAHs obtaining similar performances compared with LC-APCI-MS; conversely, electrospray ionisation (ESI) did not provide good performances. While the use of separation techniques (GC and LC) are necessary for obtaining quantitative information from the samples analysed, they may not give a complete picture of sample qualitative composition.

Direct infusion analysis with ESI-HRMS has provided a wealth of information about the chemical composition of both natural and laboratory generated samples (Kourtchev et al., 2014b; Laskin et

al., 2016, 2018; Romonosky et al., 2015). The advantages of using direct infusion analysis with soft ionisation techniques and HRMS detection are the low amount of sample required for the analysis, the fast analytical method compared with LC, and the possibility of identifying and differentiating several molecular formulas from the huge amount of compounds present in the complex mixture of organic aerosol. Conversely, the main disadvantages are that only qualitative information on sample composition may be retrieved as peak intensities are not directly related to compound concentrations and that it is not possible to distinguish between structural isomers (Kourtchev et al., 2014a; Laskin et al., 2018). Concerning PAHs, ESI does not ionise them well (Grosse and Letzel, 2007) because it requires heteroatoms in the molecular structure to efficiently form ions, and it may not provide a complete enough picture of the chemical composition of aerosol samples, thus influencing results of studies where the chemical composition is used for the parameterisation of aerosol properties (DeRieux et al., 2018). In this respect, APPI provided interesting new insights on the composition of laboratory-generated samples, especially concerning non-polar chromophores that are not ionised efficiently by ESI (DeRieux et al., 2018; Lin et al., 2018).

In the present study, we propose a fast method for the detection of PAHs, nitro-PAHs and oxy-PAHs in aerosol samples using direct infusion APPI-HRMS; we use an automatic data processing scheme for noise removal and MS peak assignments that can be used for non-target analysis of both ESI and APPI derived mass spectra; we evaluate the use of the APPI source for non-target analysis of the organic fraction of an urban aerosol; and we compare APPI and ESI sources for the analysis of urban organic aerosol in order to assess specific additional information brought by the use of the APPI source.

2 Materials and Methods

2.1 Chemicals and standard solutions

A stock standard mixture of PAHs (PAH Mix 3, Supelco, TraceCERT® grade), nitro-PAHs (9-nitroanthracene, Sigma-Aldrich®, BCR® grade; 4-nitrocatechol, Aldrich®, 97%; 4-nitrophenol, Sigma-Aldrich®, TraceCERT® grade) and oxy-PAHs (9,10-anthraquinone, Sigma-Aldrich®, PESTANAL® grade; 9-phenanthrenecarboxaldehyde, Aldrich®, 97%; 9-fluorenone, Aldrich®, 98%; 1-naphthaldehyde, Aldrich®, 95%; 9-hydroxyphenanthrene, Aldrich®, >95%; 9-hydroxyfluorene, Aldrich®, 96%) was used to optimise the analytical method after dilution in methanol/dichloromethane 1:1 (see Table S1 in the Supplementary Material for details). These standard compounds were chosen for method optimisation based on their potential importance in aerosol samples and commercial availability. The concentrations were in the range 6-133 μg/mL for PAHs, 0.6-5.3 μg/mL for nitro-PAHs and 0.13-13 μg/mL for oxy-PAHs. The solution was stored at -18 °C to prevent degradation.

Methanol (Optima™ LC/MS, Fisher Chemical) and dichloromethane (≥99.9%, CHROMASOLV™, HPLC grade) were used as solvents. Acetone (>99.5%, HPLC, Fisher Chemical) and toluene (anhydrous, 99.8%, Sigma-Aldrich) were used as dopants. Ultrapure water (purified by a Millipore MilliQ equipment), HPLC grade acetonitrile (Riedel de Haën) and methanol (VWR) were used for washing.

2.2 Aerosol Sampling

Teflon filters (PALL, fiberfilm, Ø 47 mm) were pre-treated for removing organic contaminants. Filters were washed successively with 2x20 mL of ultrapure water, 2x20 mL of acetonitrile and 2x20 mL of methanol for 30 minutes in an ultrasonic bath. Finally, filters were dried under vacuum for one hour and stored in a clean desiccator. Quartz fibre (Millipore, AQFA, Ø 47 mm) filters were decontaminated by baking them at 600 °C for 24 h as in previous studies (Kourtchev et al., 2014a, 2014b). Both Teflon and quartz fibre filters were successfully used in previous studies for aerosol

collection for the determination of PAHs and their derivatives (Davis et al., 1987; Giorio et al., 2019; Keyte et al., 2016; Kojima et al., 2010; Roper et al., 2015; Walgraeve et al., 2012).

Six $PM_{2.5}$ samples were collected (24 hours sampling time) from the 2nd to the 19th June 2014 (samples Q1 to Q3 and Q5 to Q7) and another six samples were collected from the 8th to the 14th January 2015 (samples FP1 to FP6) using the sampling facility at the Department of Chemical Sciences of the University of Padua (45.41 °N, 11.88 °E) (Giorio et al., 2017, 2013). A Zambelli Explorer Plus PM sampler was fitted with a $PM_{2.5}$ certified selector (CEN standard method UNI-EN 14907) working at a constant flow rate of 2.3 m^3/h. More details on sample collection and environmental conditions during sampling are reported in Table S2. Mass of aerosol particles collected on filters ranged between 0.5 mg to 1.1 mg for summer samples and between 2.0 and 5.6 mg for winter samples. After sampling, filters were stored at -18 °C until instrumental analysis. For each campaign, at least two filter blanks (filters pre-treated, taken to the field and stored using the same procedure as for filter samples but not mounted on the sampling device) were also produced.

2.3 Sample preparation

All glassware was cleaned using at least three washings with HPLC grade methanol before sample preparation. Filter samples and filter blanks were extracted as done in previous studies (Kourtchev et al., 2014b). Briefly, a quarter of a filter was manually cut and extracted three times with 5 mL of methanol in an ultrasonic bath at 0 °C (slurry ice) for 30 mins. The extracts were then combined and filtered through two syringe PTFE filters (ISO-Disc™, Supelco, with pore sizes of 0.45 µm and 0.22 µm) and then evaporated at 30.0±0.5 °C under a gentle nitrogen flow until a final volume of 1.0 mL. For APPI-HRMS analyses, 10% toluene was added as dopant.

158 **2.4 Instrumental analysis**

159 Instrumental analyses were performed by direct infusion into a high-resolution LTQ Orbitrap™
160 Velos mass spectrometer (Thermo Fisher, Bremen, Germany). The instrument mass resolution was
161 set at 100,000 (measured at *m/z* 400). Each sample was analysed in both positive (+) and negative (-
162) ionisation in the *m/z* ranges 100−650 and 150-900 (for both polarities), acquiring three replicates
163 for each range for 60 seconds. The acquisition was considered acceptable only if the spray resulted
164 sufficiently stable, with variations of the total ion current (TIC) profile versus time below 20%.
165 APPI analyses were performed using an Ion Max™ source (Thermo Fisher, Bremen, Germany) set
166 to work in APPI mode with a Syagen Krypton lamp emitting photons at 10.0 eV and 10.6 eV.
167 Source parameters were: temperature 200 °C, sheath gas flow 0 arbitrary units (a.u.), auxiliary gas
168 flow 5 a.u., sweep gas flow 10 a.u., capillary temperature 275 °C, S-lens RF level 60%. The
169 instrument syringe pump was used for direct infusion at a flow rate of 10 µL/min.
170 NanoESI analyses were performed using a chip-based nanoESI source TriVersa NanoMate (Advion
171 Biosciences, Ithaca NY, USA). The direct infusion nanoESI parameters in negative mode were as
172 follows: ionisation voltage 1.6 kV, back pressure 0.8 psi, capillary temperature 275 °C, S-lens RF
173 level 60%, sample volume 8 µL, and sample flow rate 200–300 nL/min. For the positive mode the
174 same parameters were used except for the ionisation voltage and the back pressure set at 1.4 kV and
175 0.3 psi, respectively.
176 The mass spectrometer (fitted with an ESI source) was calibrated before the analysis using a Pierce
177 LTQ Velos ESI Positive Ion Calibration Solution and a Pierce ESI Negative Ion Calibration
178 Solution (Thermo Scientific). The mass accuracy of the instrument was checked before the analysis
179 using the calibration solutions and was always below 0.5 ppm.
180

2.5 Data treatment

The post-run data processing for the assignment of unique molecular formulas to each *m*/*z* value was done according to the procedure described in details elsewhere (Zielinski et al., 2018). Briefly, for each instrumental acquisition a mass spectrum was obtained by averaging circa 40 single spectra (one minute of acquisition). In the generation of molecular formulas, carried out in Xcalibur 2.1 qualitative software, the following constrains on the elemental composition were applied: $1 \leq {}^{12}C \leq 75$; ${}^{13}C \leq 1$; $1 \leq {}^{1}H \leq 180$; ${}^{16}O \leq 50$; ${}^{14}N \leq 30$; ${}^{32}S \leq 2$; ${}^{34}S \leq 1$, mass tolerance 6 ppm and maximum number of formulas per peak 10. For positive nanoESI acquisitions, the presence of one sodium atom is also allowed in the molecular formula generation. Mass errors were automatically calculated and corrected on the basis of authentic standards (e.g., compounds in Table S1), known contaminants or substances likely to be present in the samples and previously confirmed via MS/MS experiments. The list of formulas associated to each peak in the MS is then filtered using a Mathematica 10 (Wolfram Research Inc., UK) code developed in house and already described elsewhere (Zielinski et al., 2018), which uses a series of heuristic rules for formula filtering, such as the nitrogen rule, double bond equivalent (DBE) and elemental ratios ($0.3 \leq H/C \leq 2.5$, $O/C \leq 2$, $N/C \leq 1.3$, $S/C \leq 0.8$), and takes into account the presence of both molecular and quasimolecular ions for APPI-HRMS data. When several formulas satisfied all restrictions within 2 ppm accuracy, the formula with the lowest mass error was selected. Only peaks with an intensity five times higher than in the filter blanks were kept. Finally, mass ranges were merged and only ions common among all replicate acquisitions were selected.

The carbon oxidation state ($\overline{OS}c$) was calculated as ($\overline{OS}c$) = 2 O/C − H/C (Kroll et al., 2011), the DBE values of the were calculated as $DBE = n_C - n_H/2 + n_N/2 + 1$ (Wozniak et al., 2008), the aromaticity index (AI) was calculated using the equation $AI = (1 + n_C - n_O - n_S - 0.5n_H)/(n_C - n_O - n_N - n_S)$ (Koch and Dittmar, 2006), where n_C, n_H, n_O, n_N, and n_S correspond to the number of carbon, hydrogen, oxygen, nitrogen, and sulfur atoms in the neutral formula, respectively.

206

3 Results and discussion

208

3.1 Optimisation of APPI-HRMS analysis for the measurement of PAHs, nitro-PAHs and oxy-PAHs in aerosol samples

Optimisation tests are summarised briefly in the following paragraphs while a full description of the tests performed and related results are reported, see section S1 for more information.

Optimisation of APPI acquisition in positive ionisation was done using a standard mixture of PAHs, nitro-PAHs and oxy-PAHs (details are reported in Table S1 in the supplementary materials). Different source temperatures from 50 to 350 ºC were tested, setting the mass range to *m*/*z* 100-650. For each temperature a series of mass spectra was recorded for 30 seconds each (~20 scans) after source stabilisation. The average and standard deviation of the total ion current (TIC) for each temperature condition and the extracted ion current (EIC) for two selected nitro-PAHs (4-nitrocatechol and 4-nitrophenol) and one oxy-PAH (4-phenanthrenecarboxaldehyde) are reported in Figure 1. The results indicated that both total ion current (TIC) values and related standard deviations increased with source temperature. Furthermore, for nitro- and oxy-PAHs signal intensities decreased at temperatures above 200-250 °C, indicating a thermal decomposition. Consequently, a temperature of 200 °C was chosen for the APPI-HRMS analysis in order to prevent the loss of nitro- and oxy-PAHs, with optimal overall sensitivity and spray stability.

225

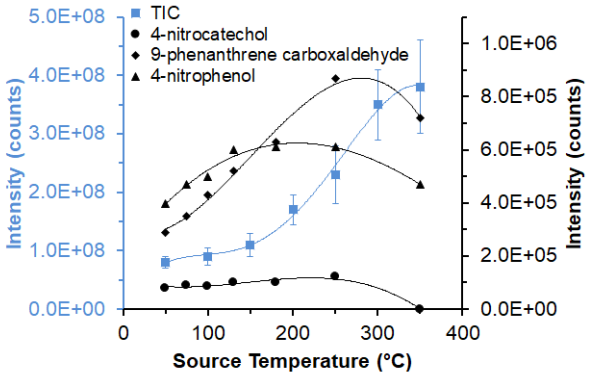

Figure 1. Total ion current (TIC) intensity trend and extracted ion current (EIC) intensity trend of selected nitro-PAHs and oxy-PAHs with the APPI source temperature showing an increase in signal variability (lower spray stability) with increasing temperature and possible degradation of nitro- and oxy-PAHs at temperatures above 200 °C.

Gas flow optimisation was done for sheath, auxiliary and sweep gasses in the range from 0 to 10 a.u.; flow rates of 5 and 10 a.u. were chosen for the auxiliary gas and the sweep gas respectively, to obtain a good compromise between response and spray stability. The sheath gas flow was turned off, as both TIC intensity and stability worsen by using it. Toluene and acetone were tested as dopant agents (Fredenhagen and Kühnöl, 2014) at concentrations of 5 and 10% (v/v). The best overall results for all compound classes were obtained by using toluene at a concentration of 10%. Discussion on individual compounds can be found in the supplementary materials, see section S1 for more information.

Optimisation of sample extraction, *via* sonication in slurry ice as in previous studies (Kourtchev et al., 2014b; Tong et al., 2016), was carried out both on blank filters spiked with PAHs, nitro-PAHs and oxy-PAHs at concentrations close to those expected in real samples (Masiol et al., 2013; Menichini, 1992; Srogi, 2007) and on a real aerosol sample. Extraction was tested with both methanol (commonly used for aerosol samples) and a methanol/dichloromethane (1:1) solution (in which unsubstituted PAHs are more soluble). It is worthwhile to underline the qualitative nature of direct infusion analysis, in which peak intensity is not strictly related to the concentration of a compound (Kourtchev et al., 2014a). This needs to be taken into consideration when drawing

conclusions from method optimisation tests and for this reason we consider as a significant difference in the recovery efficiency (calculated based on peak intensities) only a difference that is >25%. While for target analytes, in general, there were not significant differences between the use of methanol or a methanol/dichloromethane mixture (data and discussion on individual compounds can be found in the supplementary materials, see section S1 for more information), for real aerosol samples methanol showed the best performances in terms of ability to extract compounds, thus generating a larger number of detected molecular formulas. These results can be explained by a high enough solubility of target compounds in methanol (Acree, 2013) and a generally better solubility in methanol of the organic compounds present in the aerosols.

3.2 Target analysis of $PM_{2.5}$ samples

$PM_{2.5}$ samples from the summer 2014 and winter 2015 campaigns were analysed with the method developed here (direct infusion APPI(+)-HRMS) for detection of PAHs, nitro-PAHs and oxy-PAHs. Results of the analysis are summarised in Table 1 and Figure 2. Only detection of unsubstituted PAHs was compared with concentrations in $PM_{2.5}$, determined using the standardised analytical method (EN 15549:2008), obtained from ARPA Veneto, the Regional Environmental Agency, as concentrations of nitro- and oxy-PAHs are not routinely determined. Among all samples, 12 peaks were detected corresponding to molecular formulas of target PAHs, nitro-PAHs and oxy-PAHs (Figure 2). The most frequently detected peak corresponds to the molecular formula $C_{20}H_{12}$, which could be associated with benzo[a]pyrene, benzo[b]fluoranthene and benzo[k]fluoranthene, present at the highest concentrations in these sample series. As expected, summer samples were depleted in PAHs due to higher temperatures (average temperature >20 °C), faster photochemical degradation and lower emissions (Menichini, 1992).

It is worth noting that no peak was detected for $C_{18}H_{12}$, corresponding to benz[a]anthracene and chrysene, and $C_{22}H_{12}$, corresponding to benzo[ghi]perylene and indeno[1,2,3-cd]pyrene in samples

Q5, FP3 and FP5, despite they were at concentrations comparable with those of $C_{20}H_{12}$, according to the ARPA Veneto analysis (Table 1). All these isomers exhibited a low response, so that measured concentrations fall around our estimated detection limits (0.79-25 ng/m^3 for a sampled volume of 55 m^3 used in this study). In this respect even small differences in the total concentration of isomers as well as distribution in isomers with a different instrumental response (two structural isomers for $C_{18}H_{12}$, three structural isomers for $C_{20}H_{12}$ and two structural isomers for $C_{22}H_{12}$) can affect the detection ability. Another explanation for not detecting some unsubstituted PAHs in real samples could be the competitive ionisation and ion suppression that are common when analysing complex mixtures with direct infusion into an ionisation source (Laskin et al., 2018).

Table 1. Comparison between PAHs detected (blue cells, increasing darkness indicates increasing peak intensities in three levels: light-blue <10^3, blue 10^3-10^4 and dark-blue >10^4) in $PM_{2.5}$ samples from Padua (Italy) with APPI(+)-HRMS and concentrations of PAHs (numbers in the table) obtained from ARPA Veneto in ng/m^3 for samples collected in in summer 2014 and winter 2015, and in which both analyses were available.

Neutral formula	Compound	Summer samples		Winter samples	
		Q1	Q5	FP3	FP5
$C_{18}H_{12}$	Benz[a]anthracene/ Chrysene	0.06/ 0.14	0.05/ 0.11	5.39/ 4.82	4.85/ 4.23
$C_{20}H_{12}$	Benzo[b]fluoranthene/ Benzo[k]fluoranthene/ Benzo[a]pyrene	0.11/ 0.05/ 0.07	0.10/ 0.04/ 0.07	4.92/ 2.59/ 5.02	4.56/ 2.47/ 5.01
$C_{22}H_{12}$	Benzo[ghi]perylene/ Indeno[1,2,3-cd]pyrene	0.09/ 0.08	0.09/ 0.05	4.71/ 3.66	4.70/ 3.48
$C_{22}H_{14}$	Dibenz[a,h]anthracene	<0.02	<0.02	0.40	0.38

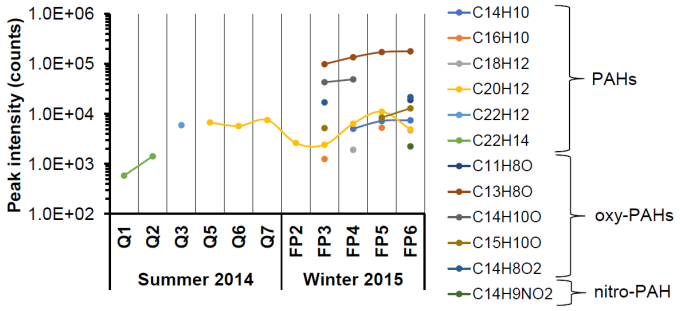

Figure 2. Peak intensities of the target PAHs, nitro-PAHs and oxy-PAHs detected with APPI(+)-HRMS in $PM_{2.5}$ samples from Padua (Italy) in summer 2014 and winter 2015 campaigns.

Indeed, the method presented here does not provide quantitative information on PAHs as opposed to classical fluorescence-based techniques, but it allows a fast detection of nitro- and oxy-PAHs that are not amenable to fluorescence detection without a labour-intensive derivatisation step (Delhomme et al., 2007). Although for non-oxidised PAHs this method would need to be improved in future studies to achieve LODs comparable with reference methods, it clearly shows that oxidised PAHs are present (Figure 2) in samples collected during the winter time when emissions of their precursors from combustion of fossil fuels and biomasses are higher. These compounds, indeed, were not detected in summer samples probably because of lower emissions of their precursors and faster degradation due to higher temperatures and stronger irradiation (see Table S2 for solar irradiance and temperature data).

In conclusion, APPI-HRMS was able to detect 12 molecular formulas corresponding to target compounds, of which six PAHs, five oxy-PAHs and one nitro-PAH.

3.3 Non-target analysis of $PM_{2.5}$ samples

All summer and winter samples were analysed with both APPI-HRMS and nanoESI-HRMS in positive and negative ionisation. The majority of the peaks in the mass spectra was below *m*/*z* 350, with only few peaks between *m*/*z* 350 and 450, and almost no peaks at *m*/*z* > 450. These results are in contrast with biogenic aerosols generated in smog chambers (Kourtchev et al., 2015, 2014a) or

311 collected in remote locations, such as the boreal forest (Kourtchev et al., 2016), where high
312 molecular weight compounds were observed under certain atmospheric conditions. Results are
313 instead in line with other studies from urban locations (Kourtchev et al., 2014b; Tong et al., 2016).
314 In order to have an overview of the results obtained with different ionisation sources and polarities,
315 the discussion is outlined considering the common ions of six summer samples (Q1, Q2, Q3, Q5,
316 Q6 and Q7) and the common ions of five winter samples (FP2, FP3, FP4, FP5 and FP6). Detailed
317 comments about sample-to-sample variability due to different environmental conditions are not the
318 focus of this study. The common ion discussion presented here is an indication of typical
319 compounds for summer and winter, respectively.
320
321 *3.3.1 Comparison between APPI-HRMS and nanoESI-HRMS*
322 ESI-HRMS is widely used for aerosol characterisation and it provides information on oxidised
323 organic component (Kourtchev et al., 2014b; Laskin et al., 2016, 2018; Romonosky et al., 2015).
324 Due to the mechanism of ion generation (Awad et al., 2015), ESI performs less well in the
325 determination of the non-polar compounds. In contrast, these compounds could be ionised with
326 APPI. Here we compare the two ionisation sources to assess what kind of information the use of
327 APPI may bring in addition to ESI for the characterisation of an urban atmospheric aerosol.
328 In nanoESI, the majority of compounds were detected as quasimolecular ions, while $[M+Na]^+$
329 adducts represented about 13% of the total molecular assignments, of which about 1% were unique
330 assignments and 12% were also detected as $[M+H]^+$, in positive ionisation mode. Concerning APPI
331 in both positive and negative ionisation modes, quasimolecular and molecular ions were about 80%
332 and 20% of the peaks detected (in number), respectively.
333 In Table 2 the number of identified molecular formulas for each compound class from both summer
334 and winter samples are reported. The main chemical information (as mean, 1st quartile and 3rd
335 quartile values) extractable from HRMS data is summarised in Table 3. In general, nanoESI

provided a larger number of formulas than APPI (see last row in Table 2). Figure 3 shows the overlap and specificity of the different ionisation sources and ionisation modes used in this study. It is worth noticing that while there is some overlap between the molecular formulas identified in the samples using the different sources and ionisation modes, the vast majority are mutually exclusive. However, while in the winter samples the number of inferred molecular formulas was comparable between the two sources, in the summer samples APPI detected 90% less molecular formulas compared with nanoESI. While the low flow rates used for nanoESI-HRMS analysis may help in increasing the overall sensitivity of the instrumental technique, this is not sufficient to explain the strong seasonal differences in detection ability. The significantly lower number of identified molecular formulas by APPI-HRMS in the summer samples could be explained instead by a limited presence of compounds that can be photoionised (see also section 3.2). This can be due to lower emissions of photoionisable compounds, their faster degradation in summer due to an increased photo-reactivity, and the non-condensation/adsorption of these compounds onto the aerosol particles due to higher temperatures.

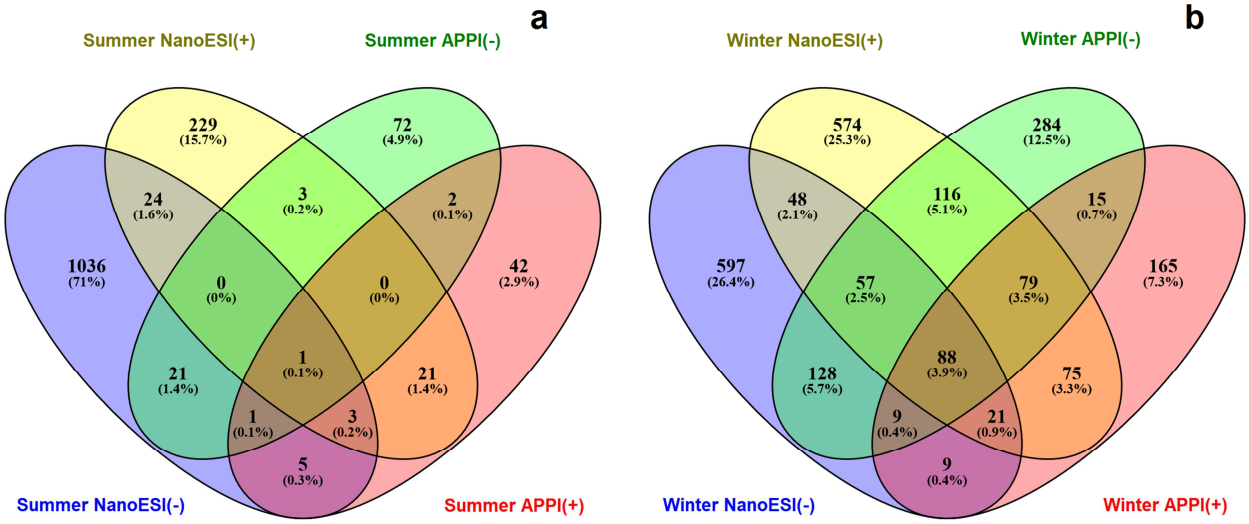

Figure 3. Venn diagrams showing the overlap and specificity of the different ionisation sources (nanoESI *vs.* APPI) and ionisation modes (positive polarity *vs.* negative polarity) used for the characterisation of both summer (a) and winter (b) samples.

Table 2. Elemental composition of $PM_{2.5}$ resulting from the common ions among six summer 2014 samples and among five winter 2015 samples, retrieved from nanoESI and APPI-HRMS analysis in both positive (+) and negative (-) ionisation.

Compound class	Number of molecular assignments and relative percentage (%)							
	Summer samples				Winter samples			
	NanoESI(+)	NanoESI(-)	APPI(+)	APPI(-)	NanoESI(+)	NanoESI(-)	APPI(+)	APPI(-)
CH	4 (0.6%)	0 (0.0%)	0 (0.0%)	0 (0.0%)	5 (0.5%)	0 (0.0%)	14 (3.0%)	0 (0.0%)
CHN	30 (4.2%)	1 (0.1%)	2 (2.7%)	11 (11.0%)	128 (12.1%)	1 (0.1%)	13 (2.8%)	68 (7.5%)
CHO	282 (39.6%)	275 (25.2%)	51 (68.0%)	28 (28.0%)	357 (33.7%)	346 (36.1%)	282 (60.5%)	421 (46.2%)
CHNO	386 (54.1%)	520 (47.7%)	16 (23.6%)	41 (41.0%)	568 (53.7%)	506 (52.8%)	153 (32.8%)	418 (45.9%)
CHNSO	11 (1.5%)	106 (9.7%)	5 (6.7%)	14 (14.0%)	0 (0.0%)	25 (2.6%)	2 (0.4%)	4 (0.4%)
CHSO	0 (0.0%)	189 (17.3%)	1 (1.3%)	5 (5.0%)	0 (0.0%)	80 (8.4%)	2 (0.4%)	0 (0.0%)
Total	713 (100%)	1091 (100%)	75 (100%)	100 (100%)	1058 (100%)	958 (100%)	466 (100%)	911 (100%)

NanoESI(+) detected CHN peaks more efficiently than APPI(+), and this fact was more evident for winter samples (12% of the molecular formulas *vs.* 3%). NanoESI(+) is sensitive to low oxidised, aliphatic compounds such as aldehydes, ketones and amines. Those compounds may be detected with APPI(+) only if they are photoionisable which is not necessarily the case. Consequently, nanoESI(+) can show higher values of H/C in the samples compared with other sources and ionisation modes (Table 3).

Table 3. Mean values (1st quartile/3rd quartile) of O/C, H/C, double bond equivalent (DBE), carbon oxidation state ($\overline{OS}c$) and aromaticity index (AI) of the data for $PM_{2.5}$ samples from summer 2014 and winter 2015

analysed with both APPI-HRMS and nanoESI-HRMS in both polarities. The largest value for each parameter is highlighted in bold.

		O/C	H/C	DBE	$\overline{OS}_c$	AI
		mean ($1^{st}/3^{rd}$ quartile)	mean ($1^{st}/3^{rd}$ quartile)	mean ($1^{st}/3^{rd}$ quartile)	mean ($1^{st}/3^{rd}$ quartile)	mean ($1^{st}/3^{rd}$ quartile)
Summer	**APPI(-)**	0.32 (0.14/0.47)	1.44 (1.14/1.72)	5.35 (3.00-8.00)	-0.81 (-1.20/-0.44)	0.44 (0.00-0.44)
	APPI(+)	0.20 (0.09/0.25)	1.55 (1.30/1.90)	4.68 (2.00/7.00)	-1.15 (-1.53/-0.88)	0.21 (0.00/0.29)
	NanoESI(-)	**0.73 (0.46/0.91)**	1.35 (1.03/1.63)	4.63 (3.00/6.00)	**0.10 (-0.35/0.5)**	0.11 (0.00-0.08)
	NanoESI(+)	0.28 (0.16/0.38)	**1.58 (1.38/1.80)**	4.13 (3.00/5.25)	-1.03 (-1.35/-0.71)	0.12 (0.00/0.20)
Winter	**APPI(-)**	0.33 (0.13/0.43)	0.99 (0.69/1.20)	**7.66 (5.00/10.00)**	-0.33 (-0.68/0.00)	**0.64 (0.00/0.69)**
	APPI(+)	0.21 (0.10/0.28)	1.28 (0.93/1.64)	6.84 (4.00/9.00)	-0.85 (-1.27/-0.47)	0.39 (0.04/0.54)
	NanoESI(-)	0.60 (0.38/0.78)	1.13 (0.88/1.33)	6.44 (4.00/8.00)	0.08 (-0.29/0.40)	0.21 (0.00/0.40)
	NanoESI(+)	0.19 (0.09/0.25)	1.21 (0.94/1.44)	7.07 (5.00/9.00)	-0.84 (-1.13/-0.56)	0.39 (0.18/0.58)

Notably, APPI(+) showed a small but significant presence of CH compounds not highlighted by nanoESI, as photoionisation does not need heteroatoms in the molecular structure to form ions, but rather favourably ionises structures with unsaturation and π-delocalisation. However, APPI(-) detected many more compounds than APPI(+), which is likely due to the presence of highly oxidised compounds in the aerosol, e.g. oxy-PAHs, that may carry functional groups promoting the ionisation in negative mode.

Both ionisation sources, in both positive and negative modes, can detect oxidised compounds. However, it is not straightforward to make hypothesis on the molecular structures corresponding to the identified molecular formulas in complex atmospheric aerosol samples. Therefore, metrics such as DBE and AI were developed. The AI is a measure of C–C double-bond density and it considers the contribution of π-bonds by heteroatoms. It has two threshold values as indicators for the

existence of aromatic (AI>0.5) and poly-aromatic compounds (AI>0.67) (Koch and Dittmar, 2006; Tong et al., 2016). AI has been shown to represent a lower limit of the actual aromaticity in a molecule. The DBE and AI descriptors goes hand in hand in this study (Table 3), with APPI(-) presenting the highest values of both descriptors in the analysed samples. Therefore, the compounds responsible for this result are most likely oxidised aromatic and poly-aromatic compounds.

Finally, nanoESI(-) is the most sensitive ionisation technique/mode for oxidised compounds, and thus, in these samples, it shows the highest values of O/C and $\overline{OSc}$ (Table 3), a particular useful metric to describe the degree of oxidation of atmospheric organic species (Kroll et al., 2011). As expected, nanoESI(-) was sensitive also to oxidised S-containing compounds (Holčapek et al., 2010). While an extensive comparison of the performances of nanoESI and APPI, in both ionisation modes, for S-containing compounds was not done, the highest detection efficiency of nanoESI(-) displayed in this study is likely interlinked with a high oxidation state of S-containing compounds in the aerosol samples.

3.3.2 Chemical characterisation and seasonality

Concerning the overall composition of summer and winter samples, CHO and CHON were the most numerous molecular formulas identified in both seasons and in all conditions of analysis (Table 2). Non-oxygenated molecular formulas, i.e. CH and CHN compounds, contributed marginally to the detected chemical composition of the samples and their contribution strongly decreased in the summer samples compared with winter samples due to enhanced photo-reactivity in the warm season and possibly lower emissions of anthropogenic precursors. Conversely, the CHSO and CHNSO groups (combined) increased from 11% of molecular formulas identified in the winter samples to 27% in the summer samples (Table 2). Organosulfates ($-SO_4$) and sulfuric acid derivatives ($-SO_3$), efficiently produced in summer season from photochemical reactions of VOCs with SO_2 (concentrations in the summer ranged between 0.7-1.2 ppb with diesel and petrol fuel use

414 for road transport likely as main sources (European Commission, 2018; Giorio et al., 2015b)) and
415 heterogeneous reactions of organic peroxides with acidic sulfate (Hettiyadura et al., 2017;
416 Kristensen and Glasius, 2011; Meagher et al., 1983; Rincón et al., 2012; Zhang et al., 2012), are
417 likely dominating these sub-classes of compounds.

418 In summer samples, the chemical profiles are characterized by larger O/C and H/C values (Table 3).
419 Figure 4 shows the $\overline{OS}c$ *vs.* number of carbon atoms in both summer and winter samples analysed
420 with nanoESI-HRMS and APPI-HRMS. Summer samples are characterised by a high data density
421 at high $\overline{OS}c$ and low carbon number (Figure 4b). The corresponding molecular formulas could be
422 related to highly oxidised compounds, better ionised by nanoESI(-), formed in the aerosol through
423 reactions of fragmentation and functionalisation, increasing the oxidation of the structures and
424 simultaneously decreasing the molecular weight. In the same samples, a high data density can be
425 observed at higher molecular weights and lower $\overline{OS}c$ (Figure 4). These identified molecular
426 formulas may be related to compounds (better ionised by nanoESI(+)) of primary biogenic origin,
427 e.g. long chain fatty acids and other components of plants' cuticle (Giorio et al., 2015a; Jetter et al.,
428 2006), which can be seen also in the zone of the Van Krevelen diagram in Figure 5 with high
429 density of data at high H/C and low O/C values, or produced in the aerosol by reactions of
430 oligomerisations, which drive the formation of high molecular weight structures, characterized by
431 lower $\overline{OS}c$ (Hall IV and Johnston, 2012; Kalberer et al., 2004; Kourtchev et al., 2015). On the other
432 hand, the number of molecular formulas identified with APPI-HRMS in summer samples is low and
433 spread on the diagram plane (Figure 4a).

434 In winter samples, APPI, especially in positive ionisation, identified a large number of molecular
435 formulas characterised by low $\overline{OS}c$ and high molecular weight (Figure 4c), thus providing additional
436 information compared with nanoESI-HRMS. The compounds generating the identified molecular
437 formulas are unlikely to be formed through oligomerisation reactions, as evidenced by the Kendrick
438 Mass Defect (KMD) plots in Figures S3 and S4, but are rather primarily emitted aromatic

compounds (see section S2 for more information). This is supported also by the results of the target analysis (section 3.2). In winter, primary emissions from biomass and fossil fuel burning are more important, producing PAHs and substituted PAHs better ionisable with APPI. AI is higher in winter samples, and especially in APPI(-), suggesting the presence of oxidised aromatic and poly-aromatic compounds in the samples.

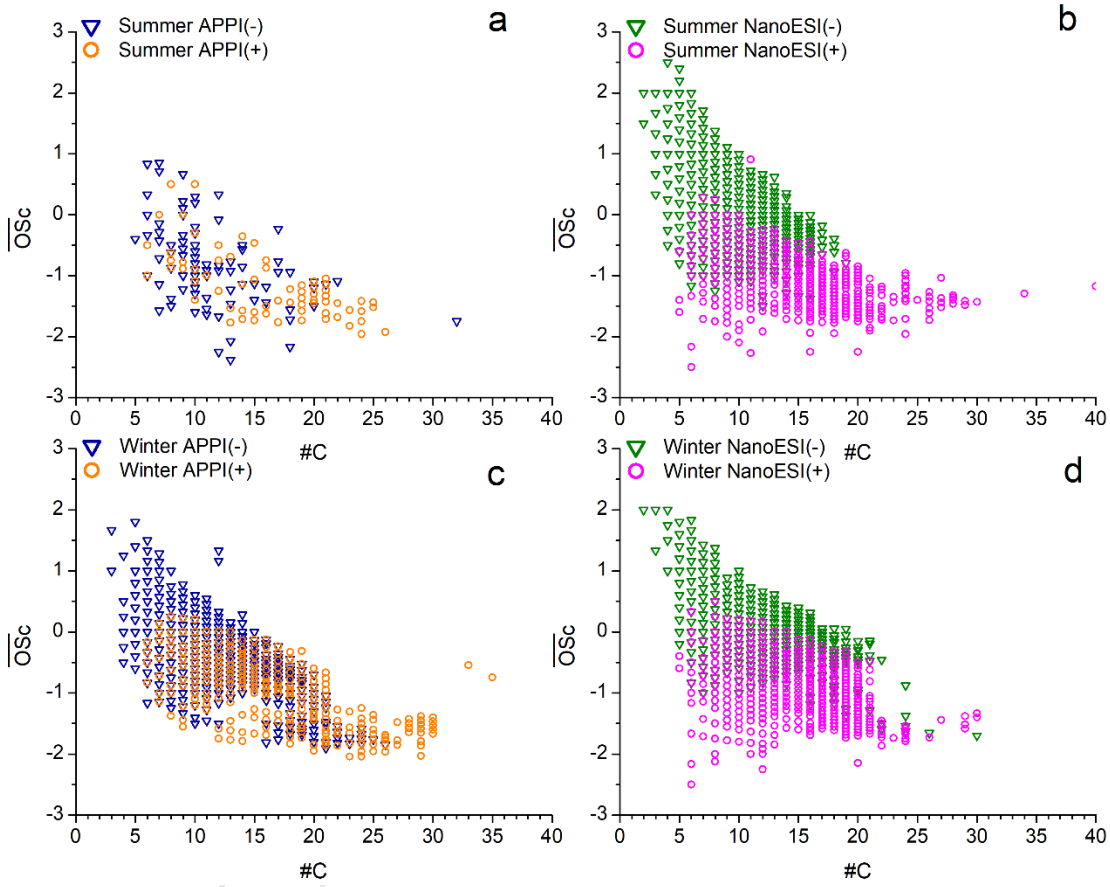

Figure 4. Carbon oxidation state ($\overline{OSc}$) *vs.* number of carbon atoms (#C) for summer samples analysed with APPI-HRMS (a) and nanoESI-HRMS (b) and for winter samples analysed with APPI-HRMS (c) and nanoESI-HRMS (d) in both negative (-) and positive (+) polarities.

This is better shown by the Van Krevelen plots reported in Figure 5, showing the AI values as a colour scale, for both summer and winter samples analysed with APPI-HRMS and nanoESI-HRMS. In general, plots for APPI-HRMS and nanoESI-HRMS exhibited the same general features (by comparing the same polarity) for the winter samples (Figure 5). APPI(-), especially in winter,

showed a markedly different feature with a high density of data in the zone of the plot with low H/C and O/C values corresponding to molecular formulas with high AI. This observation is related to the presence of a large number of aromatics (AI>0.5) and poly-aromatics (AI>0.67). Some of these aromatics are ionised also by nanoESI-HRMS in both polarities. Since the vast majority of these molecular formulas has O/C>0, the corresponding compounds can contain functional groups that can be easily ionised with nanoESI as well as with APPI.

For both ion sources, negative polarity covered a wide range of O/C values (up to 2) in both seasons, whilst positive polarity produced formulas with relatively low O/C (<1). NanoESI(+) identified a large number of formulas without oxygen, mainly CHN molecular formulas (Table 2). The area characterized by high H/C is richer in molecular formulas in the summer samples compared with the winter samples, as evidenced by nanoESI. Those formulas mainly correspond to N-containing compounds, e.g. CHNO and CHNSO, as evidenced also in previous studies in urban locations and possibly produced through photochemical oxidation reactions in the atmosphere (Kourtchev et al., 2014b; Rincón et al., 2012).

This study shows that the use of the APPI source, in addition to ESI, can bring new insights into the composition of urban atmospheric aerosols especially for non-polar and oxidised aromatic compounds that are better ionised with APPI.

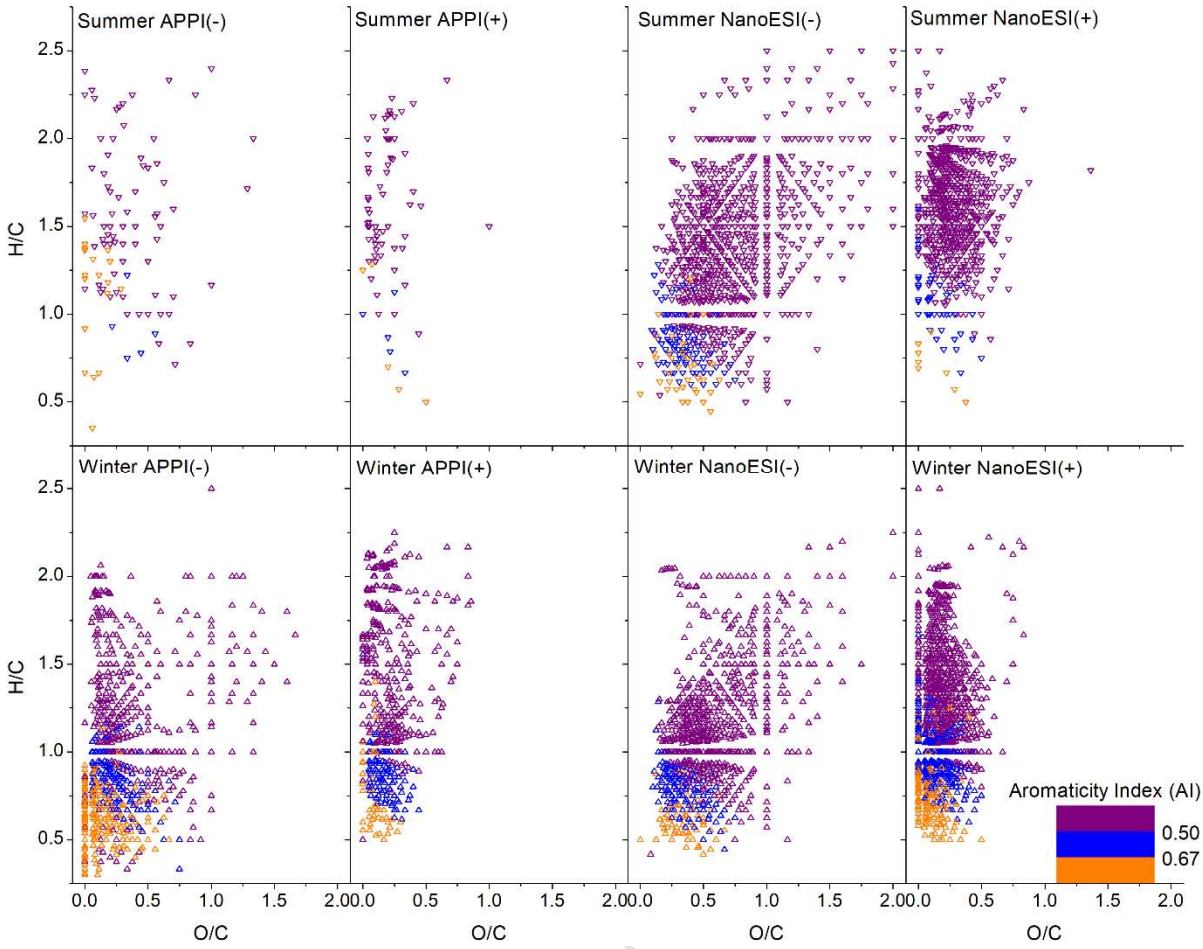

Figure 5. Van Krevelen diagrams (H/C *vs*. O/C) with Aromaticity Index (AI) values of the common ions detected in $PM_{2.5}$ samples from summer 2014 and winter 2015 analysed with APPI-HRMS and nanoESI-HRMS in both positive (+) and negative (-) polarities. AI>0.5 (purple) corresponds to non-aromatics, 0.5<AI<0.67 (blue) corresponds to mono-aromatics and AI>0.67 (orange) corresponds to poly-aromatics.

4 Conclusions

A new method has been proposed for the analysis of aerosol sample extracts by direct infusion APPI-HRMS for the determination of PAHs, nitro-PAHs and oxy-PAHs. The proposed method has been successfully applied to the analysis of $PM_{2.5}$ samples from an urban location in the northern Italian Po Valley, and it was able to detect 12 molecular formulas corresponding to target compounds, of which six PAHs, five oxy-PAHs and one nitro-PAH.

The study has then been extended to the non-target analysis of $PM_{2.5}$ samples to assess the role of the ion source (APPI *vs*. nanoESI) in depicting specific characteristics of aerosol composition.

In general, for the analysed aerosol samples, nanoESI in negative polarity was the most sensitive and provided better information on molecular formulas characterised by high O/C and $\overline{OS}c$, including those of the CHSO and CHNSO groups. In positive polarity, nanoESI can quite efficiently provide information on molecular formulas characterised by high H/C, including CHN formulas, whereas APPI was sensitive to unsaturated and especially poly-aromatic compounds, nitro- and oxy-derivatives.

APPI did not provide any additional information on the composition of summer samples that were characterised by molecular formulas possibly originated from highly oxidised organic compounds, including S-containing compounds, better ionised in nanoESI(-). Conversely, for winter samples, APPI can appreciably reveal a series of aromatic and poly-aromatic compounds, including non-substituted aromatics (CH compounds), that were not ionised with nanoESI. These compounds are better ionised in negative polarity indicating that they are aged/oxidised aromatic compounds. Thus, it is worthwhile to analyse aerosol samples with APPI, as well as with ESI, to obtain a more complete picture of the chemical composition.

Acknowledgements

This work was funded by the European Research Council (ERC starting grant 279405). Authors are grateful to Gianni Formenton (ARPA Veneto, the Environmental Regional Agency) for providing data on concentrations of PAHs and environmental conditions.

References

Acree, W.E., 2013. IUPAC-NIST Solubility Data Series. 98. Solubility of Polycyclic Aromatic Hydrocarbons in Pure and Organic Solvent Mixtures—Revised and Updated. Part 3. Neat Organic Solvents. J. Phys. Chem. Ref. Data 42, 013105. https://doi.org/10.1063/1.4775402

Adelhelm, C., Niessner, R., Pöschl, U., Letzel, T., 2008. Analysis of large oxygenated and nitrated polycyclic aromatic hydrocarbons formed under simulated diesel engine exhaust conditions

(by compound fingerprints with SPE/LC-API-MS). Anal. Bioanal. Chem. 391, 2599–2608. https://doi.org/10.1007/s00216-008-2175-9

ASTM International, 2013. ASTM D6209 - 13 Standard Test Method for Determination of Gaseous and Particulate Polycyclic Aromatic Hydrocarbons in Ambient Air (Collection on Sorbent-Backed Filters with Gas Chromatographic/Mass Spectrometric Analysis), in: Book of Standards Volume: 11.07. West Conshohocken, PA. https://doi.org/10.1520/D6209-13

Awad, H., Khamis, M.M., El-Aneed, A., 2015. Mass spectrometry, review of the basics: Ionization. Appl. Spectrosc. Rev. 50, 158–175. https://doi.org/10.1080/05704928.2014.954046

Bacaloni, A., Cafaro, C., de Giorgi, L., Ruocco, R., Zoccolillo, L., 2004. Improved Analysis of Polycyclic Aromatic Hydrocarbons in Atmospheric Particulate Matter by HPLC-Fluorescence. Ann. Chim. 94, 751–759. https://doi.org/10.1002/adic.200490093

Davis, C.S., Fellin, P., Otson, R., 1987. A Mevaew of Sampling Metliodls for Folyaromatic Hydrocarbons in Air. J. Air Pollut. Control Assoc. 37, 1397–1408. https://doi.org/10.1080/08940630.1987.10466334

Delhomme, O., Herckes, P., Millet, M., 2007. Determination of nitro-polycyclic aromatic hydrocarbons in atmospheric aerosols using HPLC fluorescence with a post-column derivatisation technique. Anal. Bioanal. Chem. 389, 1953–1959. https://doi.org/10.1007/s00216-007-1562-y

DeRieux, W.-S.W., Li, Y., Lin, P., Laskin, J., Laskin, A., Bertram, A.K., Nizkorodov, S.A., Shiraiwa, M., 2018. Predicting the glass transition temperature and viscosity of secondary organic material using molecular composition. Atmos. Chem. Phys. 18, 6331–6351. https://doi.org/10.5194/acp-18-6331-2018

EN 15549:2008, n.d. Air quality — Standard method for the measurement of the concentration of benzo[a]pyrene in ambient air.

EU, 2005. Directive 2004/107/EC of the European Parliament and of the Council of 15/12/2004 relating to arsenic, cadmium, mercury, nickel and polycyclic aromatic hydrocarbons in ambient air. Off. J. Eur. Union L 23, 3–16.

European Commission, 2018. REPORT FROM THE COMMISSION TO THE EUROPEAN PARLIAMENT AND THE COUNCIL Quality of petrol and diesel fuel used for road transport in the European Union (Reporting year 2016), https://eur-lex.europa.eu/legal-content/EN/TXT/PDF/?uri=CELEX:52018DC0056&from=EN.

Fredenhagen, A., Kühnöl, J., 2014. Evaluation of the optimization space for atmospheric pressure photoionization (APPI) in comparison with APCI. J. Mass Spectrom. 49, 727–736.

https://doi.org/10.1002/jms.3401

Giorio, C., Marton, D., Formenton, G., Tapparo, A., 2017. Formation of Metal–Cyanide Complexes in Deliquescent Airborne Particles: A New Possible Sink for HCN in Urban Environments. Environ. Sci. Technol. 51, 14107–14113. https://doi.org/10.1021/acs.est.7b03123

Giorio, C., Moyroud, E., Glover, B.J., Skelton, P.C., Kalberer, M., 2015a. Direct Surface Analysis Coupled to High-Resolution Mass Spectrometry Reveals Heterogeneous Composition of the Cuticle of Hibiscus trionum Petals. Anal. Chem. 87, 9900–9907. https://doi.org/10.1021/acs.analchem.5b02498

Giorio, C., Pizzini, S., Marchiori, E., Piazza, R., Grigolato, S., Zanetti, M., Cavalli, R., Simoncin, M., Soldà, L., Badocco, D., Tapparo, A., 2019. Sustainability of using vineyard pruning residues as an energy source: Combustion performances and environmental impact. Fuel 243, 371–380. https://doi.org/10.1016/j.fuel.2019.01.128

Giorio, C., Tapparo, A., Dall'Osto, M., Beddows, D.C.S., Esser-Gietl, J., Healy, R.M., Harrison, R.M., 2015b. Local and regional components of aerosol in a heavily trafficked street canyon in central London derived from PMF and cluster analysis of single particle ATOFMS spectra. Environ. Sci. Technol. 39, 3330–3340. https://doi.org/10.1021/es506249z

Giorio, C., Tapparo, A., Scapellato, M.L., Carrieri, M., Apostoli, P., Bartolucci, G.B., 2013. Field comparison of a personal cascade impactor sampler, an optical particle counter and CEN-EU standard methods for PM10, PM2.5 and PM1 measurement in urban environment. J. Aerosol Sci. 65, 111–120. https://doi.org/10.1016/j.jaerosci.2013.07.013

Grosse, S., Letzel, T., 2007. Liquid chromatography/atmospheric pressure ionization mass spectrometry with post-column liquid mixing for the efficient determination of partially oxidized polycyclic aromatic hydrocarbons. J. Chromatogr. A 1139, 75–83. https://doi.org/10.1016/j.chroma.2006.10.086

Hall IV, W.A., Johnston, M. V, 2012. Oligomer formation pathways in secondary organic aerosol from MS and MS/MS measurements with high mass accuracy and resolving power. J. Am. Soc. Mass Spectrom. 23, 1097–1108. https://doi.org/10.1007/s13361-012-0362-6

Hettiyadura, A.P.S., Jayarathne, T., Baumann, K., Goldstein, A.H., de Gouw, J.A., Koss, A., Keutsch, F.N., Skog, K., Stone, E.A., 2017. Qualitative and quantitative analysis of atmospheric organosulfates in Centreville, Alabama. Atmos. Chem. Phys. 17, 1343–1359. https://doi.org/10.5194/acp-17-1343-2017

Holčapek, M., Jirásko, R., Lísa, M., 2010. Basic rules for the interpretation of atmospheric pressure ionization mass spectra of small molecules. J. Chromatogr. A 1217, 3908–3921.

578 https://doi.org/10.1016/j.chroma.2010.02.049
579 Jetter, R., Kunst, L., Samuels, A.L., 2006. Composition of plant cuticular waxes, in: Riederer, M.,
580 Müller, C. (Eds.), Annual Plant Reviews Volume 23: Biology of the Plant Cuticle. Blackwell
581 Publishing Ltd, Oxford, UK, pp. 145–181. https://doi.org/10.1002/9780470988718.ch4
582 Kalberer, M., Paulsen, D., Sax, M., Steinbacher, M., Dommen, J., Prévôt, A.S.H., Fisseha, R.,
583 Weingartner, E., Frankevich, V., Zenobi, R., Baltensperger, U., 2004. Identification of
584 polymers as major components of atmospheric organic aerosols. Science 303, 1659–62.
585 https://doi.org/10.1126/science.1092185
586 Keyte, I.J., Albinet, A., Harrison, R.M., 2016. On-road traffic emissions of polycyclic aromatic
587 hydrocarbons and their oxy- and nitro- derivative compounds measured in road tunnel
588 environments. Sci. Total Environ. 566–567, 1131–1142.
589 https://doi.org/10.1016/j.scitotenv.2016.05.152
590 Kim, K.-H., Kabir, E., Kabir, S., 2015. A review on the human health impact of airborne particulate
591 matter. Environ. Int. 74, 136–143. https://doi.org/10.1016/j.envint.2014.10.005
592 Koch, B.P., Dittmar, T., 2006. From mass to structure: an aromaticity index for high-resolution
593 mass data of natural organic matter. Rapid Commun. Mass Spectrom. 20, 926–932.
594 https://doi.org/10.1002/rcm.2386
595 Kojima, Y., Inazu, K., Hisamatsu, Y., Okochi, H., Baba, T., Nagoya, T., 2010. COMPARISON OF
596 PAHS, NITRO-PAHS AND OXY-PAHS ASSOCIATED WITH AIRBORNE
597 PARTICULATE MATTER AT ROADSIDE AND URBAN BACKGROUND SITES IN
598 DOWNTOWN TOKYO, JAPAN. Polycycl. Aromat. Compd. 30, 321–333.
599 https://doi.org/10.1080/10406638.2010.525164
600 Kourtchev, I., Doussin, J.-F., Giorio, C., Mahon, B., Wilson, E.M., Maurin, N., Pangui, E.,
601 Venables, D.S., Wenger, J.C., Kalberer, M., 2015. Molecular composition of fresh and aged
602 secondary organic aerosol from a mixture of biogenic volatile compounds: a high-resolution
603 mass spectrometry study. Atmos. Chem. Phys. 15, 5683–5695. https://doi.org/10.5194/acp-15-
604 5683-2015
605 Kourtchev, I., Fuller, S.J., Giorio, C., Healy, R.M., Wilson, E., O'Connor, I.P., Wenger, J.C.,
606 McLeod, M., Aalto, J., Ruuskanen, T.M., Maenhaut, W., Jones, R., Venables, D.S., Sodeau,
607 J.R., Kulmala, M., Kalberer, M., 2014a. Molecular composition of biogenic secondary organic
608 aerosols using ultrahigh-resolution mass spectrometry: comparing laboratory and field studies.
609 Atmos. Chem. Phys. 14, 2155–2167. https://doi.org/10.5194/acp-14-2155-2014
610 Kourtchev, I., Giorio, C., Manninen, A., Wilson, E., Mahon, B., Aalto, J., Kajos, M., Venables, D.,

Ruuskanen, T., Levula, J., Loponen, M., Connors, S., Harris, N., Zhao, D., Kiendler-Scharr, A., Mentel, T., Rudich, Y., Hallquist, M., Doussin, J.-F., Maenhaut, W., Bäck, J., Petäjä, T., Wenger, J., Kulmala, M., Kalberer, M., 2016. Enhanced Volatile Organic Compounds emissions and organic aerosol mass increase the oligomer content of atmospheric aerosols. Sci. Rep. 6, 35038. https://doi.org/10.1038/srep35038

Kourtchev, I., O'Connor, I.P., Giorio, C., Fuller, S.J., Kristensen, K., Maenhaut, W., Wenger, J.C., Sodeau, J.R., Glasius, M., Kalberer, M., 2014b. Effects of anthropogenic emissions on the molecular composition of urban organic aerosols: An ultrahigh resolution mass spectrometry study. Atmos. Environ. 89, 525–532. https://doi.org/10.1016/j.atmosenv.2014.02.051

Kristensen, K., Glasius, M., 2011. Organosulfates and oxidation products from biogenic hydrocarbons in fi ne aerosols from a forest in North West Europe during spring. Atmos. Environ. 45, 4546–4556. https://doi.org/10.1016/j.atmosenv.2011.05.063

Kroll, J.H., Donahue, N.M., Jimenez, J.L., Kessler, S.H., Canagaratna, M.R., Wilson, K.R., Altieri, K.E., Mazzoleni, L.R., Wozniak, A.S., Bluhm, H., Mysak, E.R., Smith, J.D., Kolb, C.E., Worsnop, D.R., 2011. Carbon oxidation state as a metric for describing the chemistry of atmospheric organic aerosol. Nat. Chem. 3, 133–9. https://doi.org/10.1038/nchem.948

Laskin, A., Gilles, M.K., Knopf, D.A., Wang, B., China, S., 2016. Progress in the Analysis of Complex Atmospheric Particles. Annu. Rev. Anal. Chem. 9, 117–143. https://doi.org/10.1146/annurev-anchem-071015-041521

Laskin, A., Laskin, J., Nizkorodov, S.A., 2015. Chemistry of Atmospheric Brown Carbon. Chem. Rev. 115, 4335–4382. https://doi.org/10.1021/cr5006167

Laskin, J., Laskin, A., Nizkorodov, S.A., 2018. Mass Spectrometry Analysis in Atmospheric Chemistry. Anal. Chem. 90, 166–189. https://doi.org/10.1021/acs.analchem.7b04249

Lim, H., Ahmed, T.M., Bergvall, C., Westerholm, R., 2013. Automated clean-up, separation and detection of polycyclic aromatic hydrocarbons in particulate matter extracts from urban dust and diesel standard reference materials using a 2D-LC/2D-GC system. Anal. Bioanal. Chem. 405, 8215–8222. https://doi.org/10.1007/s00216-013-7222-5

Lin, P., Fleming, L.T., Nizkorodov, S.A., Laskin, J., Laskin, A., 2018. Comprehensive Molecular Characterization of Atmospheric Brown Carbon by High Resolution Mass Spectrometry with Electrospray and Atmospheric Pressure Photoionization. Anal. Chem. 90, 12493–12502. https://doi.org/10.1021/acs.analchem.8b02177

Masiol, M., Formenton, G., Pasqualetto, A., Pavoni, B., 2013. Seasonal trends and spatial variations of PM10-bounded polycyclic aromatic hydrocarbons in Veneto Region, Northeast Italy.

644 Atmos. Environ. 79, 811–821. https://doi.org/10.1016/j.atmosenv.2013.07.025
645 Meagher, J.F., Bailey, E.M., Luria, M., 1983. The seasonal variation of the atmospheric SO_2 to SO_4^{2-}
646 conversion rate. J. Geophys. Res. 88, 1525. https://doi.org/10.1029/JC088iC02p01525
647 Menichini, E., 1992. Urban air pollution by polycyclic aromatic hydrocarbons: levels and sources of
648 variability. Sci. Total Environ. 116, 109–135. https://doi.org/10.1016/0048-9697(92)90368-3
649 Niederer, M., 1998. Determination of polycyclic aromatic hydrocarbons and substitutes (nitro-,
650 Oxy-PAHs) in urban soil and airborne particulate by GC-MS and NCI-MS/MS. Environ. Sci.
651 Pollut. Res. Int. 5, 209–216. https://doi.org/10.1007/BF02986403
652 Nyiri, Z., Novák, M., Bodai, Z., Szabó, B.S., Eke, Z., Záray, G., Szigeti, T., 2016. Determination of
653 particulate phase polycyclic aromatic hydrocarbons and their nitrated and oxygenated
654 derivatives using gas chromatography–mass spectrometry and liquid chromatography–tandem
655 mass spectrometry. J. Chromatogr. A 1472, 88–98.
656 https://doi.org/10.1016/j.chroma.2016.10.021
657 Rincón, A.G., Calvo, A.I., Dietzel, M., Kalberer, M., 2012. Seasonal differences of urban organic
658 aerosol composition - an ultra-high resolution mass spectrometry study. Environ. Chem. 9,
659 298–319. https://doi.org/10.1071/EN12016
660 Romonosky, D.E., Laskin, A., Laskin, J., Nizkorodov, S.A., 2015. High-Resolution Mass
661 Spectrometry and Molecular Characterization of Aqueous Photochemistry Products of
662 Common Types of Secondary Organic Aerosols. J. Phys. Chem. A 119, 2594–2606.
663 https://doi.org/10.1021/jp509476r
664 Roper, C., Chubb, L.G., Cambal, L., Tunno, B., Clougherty, J.E., Mischler, S.E., 2015.
665 Characterization of ambient and extracted PM 2.5 collected on filters for toxicology
666 applications. Inhal. Toxicol. 27, 673–681. https://doi.org/10.3109/08958378.2015.1092185
667 Srogi, K., 2007. Monitoring of environmental exposure to polycyclic aromatic hydrocarbons: a
668 review. Environ. Chem. Lett. 5, 169–195. https://doi.org/10.1007/s10311-007-0095-0
669 Stracquadanio, M., Apollo, G., Trombini, C., 2007. A study of PM2.5 and PM2.5-associated
670 polycyclic aromatic hydrocarbons at an urban site in the Po Valley (Bologna, Italy). Water.
671 Air. Soil Pollut. 179, 227–237. https://doi.org/10.1007/s11270-006-9227-6
672 Stracquadanio, M., Trombini, C., 2006. Gas to particle (PM10) partitioning of polycyclic aromatic
673 hydrocarbons (PAHs) in a typical urban environment of the Po Valley (Bologna, Italy).
674 FRESENIUS Environ. Bull. 15, 1276–1286.
675 Tong, H., Kourtchev, I., Pant, P., Keyte, I.J., O'Connor, I.P., Wenger, J.C., Pope, F.D., Harrison,
676 R.M., Kalberer, M., 2016. Molecular composition of organic aerosols at urban background and

677 road tunnel sites using ultra-high resolution mass spectrometry. Faraday Discuss. 189, 51–68.
678 https://doi.org/10.1039/C5FD00206K
679 Valotto, G., Rampazzo, G., Gonella, F., Formenton, G., Ficotto, S., Giraldo, G., 2017. Source
680 apportionment of PAHs and n-alkanes bound to PM1collected near the Venice highway. J.
681 Environ. Sci. (China) 54, 77–89. https://doi.org/10.1016/j.jes.2016.05.025
682 Walgraeve, C., Demeestere, K., De Wispelaere, P., Dewulf, J., Lintelmann, J., Fischer, K., Van
683 Langenhove, H., 2012. Selective accurate-mass-based analysis of 11 oxy-PAHs on
684 atmospheric particulate matter by pressurized liquid extraction followed by high-performance
685 liquid chromatography and magnetic sector mass spectrometry. Anal. Bioanal. Chem. 402,
686 1697–1711. https://doi.org/10.1007/s00216-011-5568-0
687 Wozniak, A.S., Bauer, J.E., Sleighter, R.L., Dickhut, R.M., Hatcher, P.G., 2008. Technical Note:
688 Molecular characterization of aerosol-derived water soluble organic carbon using ultrahigh
689 resolution electrospray ionization Fourier transform ion cyclotron resonance mass
690 spectrometry. Atmos. Chem. Phys. 8, 5099–5111. https://doi.org/10.5194/acp-8-5099-2008
691 Zhang, H., Worton, D.R., Lewandowski, M., Ortega, J., Rubitschun, C.L., Park, J.-H., Kristensen,
692 K., Campuzano-Jost, P., Day, D.A., Jimenez, J.L., Jaoui, M., Offenberg, J.H., Kleindienst,
693 T.E., Gilman, J., Kuster, W.C., de Gouw, J., Park, C., Schade, G.W., Frossard, A.A., Russell,
694 L., Kaser, L., Jud, W., Hansel, A., Cappellin, L., Karl, T., Glasius, M., Guenther, A.,
695 Goldstein, A.H., Seinfeld, J.H., Gold, A., Kamens, R.M., Surratt, J.D., 2012. Organosulfates as
696 Tracers for Secondary Organic Aerosol (SOA) Formation from 2-Methyl-3-Buten-2-ol (MBO)
697 in the Atmosphere. Environ. Sci. Technol. 46, 9437–9446. https://doi.org/10.1021/es301648z
698 Zhang, R., Wang, G., Guo, S., Zamora, M.L., Ying, Q., Lin, Y., Wang, W., Hu, M., Wang, Y.,
699 2015. Formation of Urban Fine Particulate Matter. Chem. Rev. 115, 3803–3855.
700 https://doi.org/10.1021/acs.chemrev.5b00067
701 Zielinski, A.T., Kourtchev, I., Bortolini, C., Fuller, S.J., Giorio, C., Popoola, O.A.M., Bogialli, S.,
702 Tapparo, A., Jones, R.L., Kalberer, M., 2018. A new processing scheme for ultra-high
703 resolution direct infusion mass spectrometry data. Atmos. Environ. 178, 129–139.
704 https://doi.org/10.1016/j.atmosenv.2018.01.034
705

Highlights - up to 5 bullet points (maximum 85 characters, including spaces, per bullet point)

- Determination of particle-bound PAHs, nitro-PAHs and oxy-PAHs in $PM_{2.5}$ samples
- Comparison between nanoESI and APPI sources in HRMS
- Automatic data processing scheme for both nanoESI and APPI-HRMS data
- APPI did not add information for highly oxidised organic compounds compared to nanoESI
- APPI(-) can highlight oxidised and nitrogenated PAHs better than nanoESI